In Vitro Pluripotent Stem Cell Differentiation to Hepatocyte Ceases Further Maturation at an Equivalent Stage of E15 in Mouse Embryonic Liver Development

Ravali Raju,[1,2] David Chau,[1–3] Tineke Notelaers,[4,5] Chad L. Myers,[6]
Catherine M. Verfaillie,[4,5] and Wei-Shou Hu[1,2]

Hepatocyte-like cells (HLCs) can be derived from pluripotent stem cells (PSCs) by sequential treatment of chemical cues to mimic the microenvironment of embryonic liver development. However, these HLCs do not reach the full maturity level of primary hepatocytes. In this study, we carried out a meta-analysis of cross-species transcriptome data of in vitro differentiation of human PSCs to HLCs and in vivo mouse embryonic liver development to identify the developmental stage at which HLC maturation was blocked at. Systematic variations were found associated with the data source and removed by batch correction. Using principal component analysis, HLCs from different stages of differentiation were aligned with mouse embryonic liver development chronologically. A "unified developmental time" (DT) scale was developed after aligning in vitro HLC differentiation and in vivo embryonic liver development. HLCs were found to cease further maturation at an equivalent stage of mouse embryonic day (E)13–15. Genes with discordant time dynamics were identified by aligning in vivo and in vitro data set onto a common DT scale. These genes may be targets of genetic intervention for enhancing the maturity of PSC-derived HLCs.

Keywords: hepatic differentiation, meta-analysis, gene expression, stem cells

Introduction

HEPATOCYTES DERIVED FROM pluripotent stem cells (PSCs) hold the potential of transforming the treatment of many liver diseases. They may also serve as a virtually unlimited cell source for drug toxicity and pharmacokinetics studies [1]. By culturing PSCs in different combinations of growth factors that mimic the biochemical environment during embryonic liver development, they can be directed to differentiate toward the hepatic lineage [2,3]. These differentiated cells exhibit many functional characteristics of primary hepatocytes, including albumin secretion, certain cytochrome *P450* activities, and urea synthesis. Engraftment of cells into animals has also been observed when transplanted under selective conditions [4–8].

However, despite the capability of expressing some hepatic genes, the differentiated cells are regarded as "hepatocyte-like" cells (HLCs), as many mature liver markers are either not expressed or expressed at very low levels. The general lack of maturity of HLCs was further revealed in a microarray transcriptome study showing that HLCs derived from three separate laboratories were clustered distinctively from primary hepatocytes [9]. Through functional activities and proteomic analysis, it was clearly demonstrated that HLCs were closer to fetal liver hepatocytes than primary hepatocytes [9,10].

Many approaches have been explored to enhance maturation of HLCs, including the formation of tissue-like three-dimensional (3D) structure [11,12], coculture of HLCs and endothelial cells [12–14], the addition of small molecules uncovered by screening [15–17], and overexpression of certain transcription factors (TFs) [18–20]. Nevertheless, the derivation of mature hepatocytes from PSCs is still elusive. Although the lack of maturity of HLCs has been well recognized, the stage of embryonic liver development that HLCs are equivalent to is not known. By identifying the

---

[1]Department of Chemical Engineering and Materials Science, University of Minnesota, Minneapolis, Minnesota.
[2]Stem Cell Institute, University of Minnesota, Minneapolis, Minnesota.
[3]Department of Biomedical Engineering, University of Minnesota, Minneapolis, Minnesota.
[4]Department of Development and Regeneration, KU Leuven, Leuven, Belgium.
[5]Stem Cell Institute Leuven, KU Leuven, Leuven, Belgium.
[6]Department of Computer Science and Engineering, University of Minnesota, Minneapolis, Minnesota.

developmental stage that HLC maturation is arrested at, one can begin to devise strategies to overcome the genetic roadblocks.

Human gestation occurs over 280 days compared to 20 days for mouse. Although these processes differ in time scales, they share similar progression through the different developmental stages (Supplementary Fig. S1A; Supplementary Data are available online at www.liebertpub.com/scd). A typical directed hepatocyte differentiation for both human and mouse PSCs (hPSCs and mPSCs) lasts for about 20 days [21].

We hypothesize that the transcriptome data of in vitro hepatic differentiation bear the characteristics of embryonic liver development. We set out to align the transcriptome data of different stages of HLC differentiation to those of various gestation stages of embryonic liver development. We will then identify the corresponding embryo development stage that HLC differentiation is blocked at, and uncover the discordant gene expression between the in vitro HLC differentiation and in vivo liver development that may contribute to the differentiation block.

To better understand the genetics hurdles that need to be addressed, we performed a comprehensive meta-analysis of publicly available gene expression data sets along with our own transcriptome data performed for this study. However, the transcriptome data across different stages of liver development are available only for rodents, but not humans. We hypothesized that the transcriptome dynamics of embryonic liver development between rodents and humans are highly similar, and are performed cross-species and cross-in vitro-in vivo analysis with the aim of aligning the human hepatocyte-like cell (hHLC) differentiation and the mouse embryonic liver development process onto a common scale or a "unified developmental time" (DT).

It has been reported that data obtained with different measurement platforms can often bear systematic variations and random errors [22–24]. The ComBat algorithm employs empirical Bayes method to perform a location and scale adjustment by pooling information across each gene in every batch to center the data to an overall grand mean [22]. This technique can be applied to multiple batches of data sets and is robust for small sample sizes to overcome the biasing that is typically observed [22]. Other methods of batch correction have also been reported. Some, such as the *limma* package in R, were reported to give less "exaggerated" findings [25].

However, ComBat has been used often and shown to outperform the common batch correction techniques, including distance-weighted discrimination, which uses a support vector machine-based approach [26], mean-centering (PAMR), which relies on gene-based analysis of variance [23], and surrogate variable analysis, which uses a combination of single value decomposition and linear model analysis [24,27]. Hence, we used the ComBat algorithm to integrate transcriptome data at different time points of hHLC differentiations and mouse embryonic liver development.

In this study, we seek to identify the equivalent embryonic liver development stage of HLCs. Regardless of the source and the protocol used, HLCs stop the maturation process at the same stage. We also identified genes that have different expression dynamics between in vitro differentiation and embryonic liver development. To the best of our knowledge, this is the first described meta-analysis of highly heterogeneous transcriptome data from human and mouse.

This study gives further clues for advancing directed differentiation of PSCs to hepatocytes.

Materials and Methods

Human embryonic stem cell culture

The human embryonic stem cell (hESC) line H9 was cultured using 80% Knockout™ Dulbecco's modified Eagle's medium (DMEM) (Gibco/BRL, USA), supplemented with 20% Knockout Serum Replacement (Gibco), 2.0 mM glutamine, 1×nonessential amino acids (Gibco), 55 µM β-mercaptoethanol, and 10 ng/mL basic fibroblast growth factor (FGF2). The cells were cultured on irradiated E13–14 CF-1 mouse embryonic fibroblasts (Charles River Laboratories, Wilmington, MA) at 37°C in 10% CO_2. The cells were passaged after they reached 70%–80% confluency using 0.1% (w/V) collagenase type IV (Gibco) in Knockout DMEM.

Hepatocyte differentiation

H9 and mouse induced pluripotent stem cells (miPSCs) were passaged onto 2% Matrigel®-coated plates in mTESR™ medium (Stem Cell Technologies) for 24 h or until 50%–70% confluency. Differentiation was initiated by switching to a differentiation medium, which consisted of 60/40 (v/v) mixture of low glucose DMEM (Gibco) and MCDB-201 (Sigma), supplemented with 26 µg/mL ascorbic acid 3-phosphate (Sigma). 2.5 µg/mL linoleic acid, 0.25 mg/mL bovine serum albumin, insulin-transferrin-selenium (Sigma) (2.5 µg/mL insulin, 1.38 µg/mL transferrin, and 1.25 ng/mL sodium selenite), 0.4ug/mL dexamethasone (Sigma), 4.3 µg/mL β-mercaptoethanol (Hyclone), 100 IU/mL penicillin, and 100ug/mL streptomycin (Gibco). Two percent (v/v) fetal bovine serum albumin (Hyclone) was added to the media for the first 6 days and then 0.5% (v/v) for the remaining 14 days. The differentiation medium was supplemented with stage-specific growth factors and cultured at 21% O_2 and 5% CO_2 following a previously published study [2].

Data sets

The source of human and mouse data sets are listed in Supplementary Tables S1 and S2, respectively. The human data set consisted of transcriptome of different hESCs differentiating to hepatocytes, including HLCs generated using various protocols, two time course data from different protocols (Hu/Duncan) [3,28–31], HLCs in 3D spheroids [11], liver organoids generated through coculture of induced pluripotent stem cell (iPSC)-derived HLCs and mesenchymal and endothelial cells [12], and induced hepatocytes (iHEPs) generated through direct reprogramming of fibroblasts to HLCs by hepatic TF transduction [32]. Also included were primary human hepatocytes (PHHs) (pooled messenger RNA after 1 day of culture), fetal liver (18 weeks of gestation) and adult liver. Transcriptome data of mouse embryonic liver development (E9.5 to postnatal) include CD45⁻ Ter119⁻ liver cells from C57/BL6/Tg mice embryos and whole livers from C57/B6 mice embryos [12,33].

Microarray sample processing

Total RNA was extracted at different stages during hPSC and mPSC differentiation to HLCs using the RNeasy Mini Kit

(Qiagen). Differentiating hESC (H9, HSF6) samples were hybridized to the Illumina HT12 bead array v3 (Illumina, Inc.), HES3 samples were hybridized to Human Genome U133 v2 array (Affymetrix), and the miPSC-derived samples were hybridized to the WG-6 v2 (Illumina) array.

Data analysis

Global analysis to elucidate trends in the data was performed using hierarchical clustering, principal component analysis (PCA), and non-negative matrix factorization (NMF). Before subjecting the data to batch correction, genes with static expression profiles in the data set were removed. Only those genes changing greater than fourfold across any timewise comparison were retained in the global analysis. All analysis was carried out in the statistical software, R. Briefly, the VirtualArray package in R was used to obtain Probe IDs among different samples from different microarray platforms [34]. The BioMart package in R was used to convert probe IDs to common ENSEMBL IDs among the different platforms in the expression data set [35]. Further details regarding each statistical analysis as well as the treatment of data sets of hHLC/mouse hepatocyte-like cell (mHLC) and mouse embryonic liver from the meta-analysis are described more in detail in the Supplementary Materials and Methods section.

Results

Compilation of human in vitro hepatic differentiation data

hESCs were differentiated toward the hepatic lineage using a four-stage hepatic differentiation protocol (Supplementary Fig. S1A). The transcript of hepatic markers, *HNF4A*, *AFP*, *ALB*, *CYP3A4*, *AAT*, and *TAT*, increased significantly by the end of the differentiation (Supplementary Fig. S1B). Immunohistochemistry reveals that a majority of cells were positive for endodermal marker *FOXA2* by day 6. Hepatic markers *HNF4A*, *AAT*, and *ALB* were prominent in cells by day 20 (Supplementary Fig. S1C). The high transcript expression of AFP, which is low in primary hepatocytes, suggests the fetal nature of hHLCs derived from PSCs. Samples over the course of the differentiation on days 6, 10, 14, and 20 (labeled D6_H, D10_H, D14_H, and D20_H, respectively) were collected for transcriptome assay.

The transcriptome data, along with another set of hHLC differentiation [36], and additional data from the public domain were combined together to increase the data diversity (the sources and references along with sample annotations are listed in Supplementary Table S1). One data set consisted of multiple time points over the course of differentiation from hPSCs to hHLCs (Duncan) [28], while the others consisted of hHLC samples obtained using various differentiation methods. This compilation resulted in a total of 17,683 genes that were common among all the data sets based on ENSEMBL ID.

Batch correction of human in vitro data

Batch correction was performed on the hHLC in vitro data set to remove the systematic bias caused by the heterogeneous samples and platform sources. The effect of batch correction

is visible after performing hierarchical clustering of the different samples before and after batch correction. Without batch correction, samples obtained from each study clustered together, as seen in Supplementary Figure S2. After batch correction, samples based on their similarity in differentiation stages clustered together, regardless of the study it came from, suggesting the removal of batch effects (Fig. 1A).

Samples from a similar differentiation stage for both of the time series studies (Hu/Duncan) clustered together, indicating a similar progression through the differentiation stages in different protocols. However, the hHLC data from all sources consistently clustered separately from tissue samples of fetal and adult liver samples, confirming the immaturity of these cells.

NMF analysis was performed to separate the hHLC data set into three clusters (Fig. 1B). The optimal number of clusters, three, was determined by the highest cophenetic coefficient obtained (Supplementary Fig. S3). The smallest cluster consisted of mature hepatic samples from liver tissue and primary hepatocytes, and the other two clusters consisted of samples from early (D4–10) and late differentiation (D14–20) stages. Only two hHLC samples [11,31] were grouped separately in the mature cluster. The grouping of early and late differentiation samples was remarkably similar between NMF and hierarchical clustering. Notably, samples in similar differentiation stages from the two differentiation time series studies (Hu/Duncan) were clustered together.

We used Database for Annotation, Visualization, and Integrated Discovery (DAVID) to probe the functional class of the 967 metagenes identified from the NMF analysis (Supplementary Table S3) [37]. Genes associated with the clustering of early differentiating cell states (D4–10) were involved mainly in developmental processes, while those associated with late differentiation states (D14–20) were mainly involved in cell differentiation, adhesion, extracellular matrix reorganization, epithelial specification, and drug response. The metagenes classifying fetal and adult liver tissue were involved in mature liver functions, including *CYP450* drug detoxification, electron carrier activity, and carbohydrate metabolism, among many others.

Thus, the two unsupervised classification methods, hierarchical clustering and NMF, classified the batch corrected human transcriptome data into similar groups based on the functional relevance of gene expression patterns. This gives credence to the data processing method we adopted for batch correction to further carry out the meta-analysis.

Alignment of human in vitro data along a differentiation scale

The batch corrected transcriptome data of the hHLC data set was subjected to PCA. Two principal components, PC1 and PC2, captured 90% of the data variance, suggesting that two components were sufficient to display the variability within the transcriptome data of the samples. When plotted, all samples, starting from endodermal cells to hHLCs, were observed to align chronologically along an arc, while primary hepatocytes and adult liver were in the high PC2 region (Fig 1C). The samples from the time series studies (Hu/Duncan) both aligned from left to right in chronological order based on the differentiation stages. All hHLC samples, regardless of the laboratory and protocol used, aligned
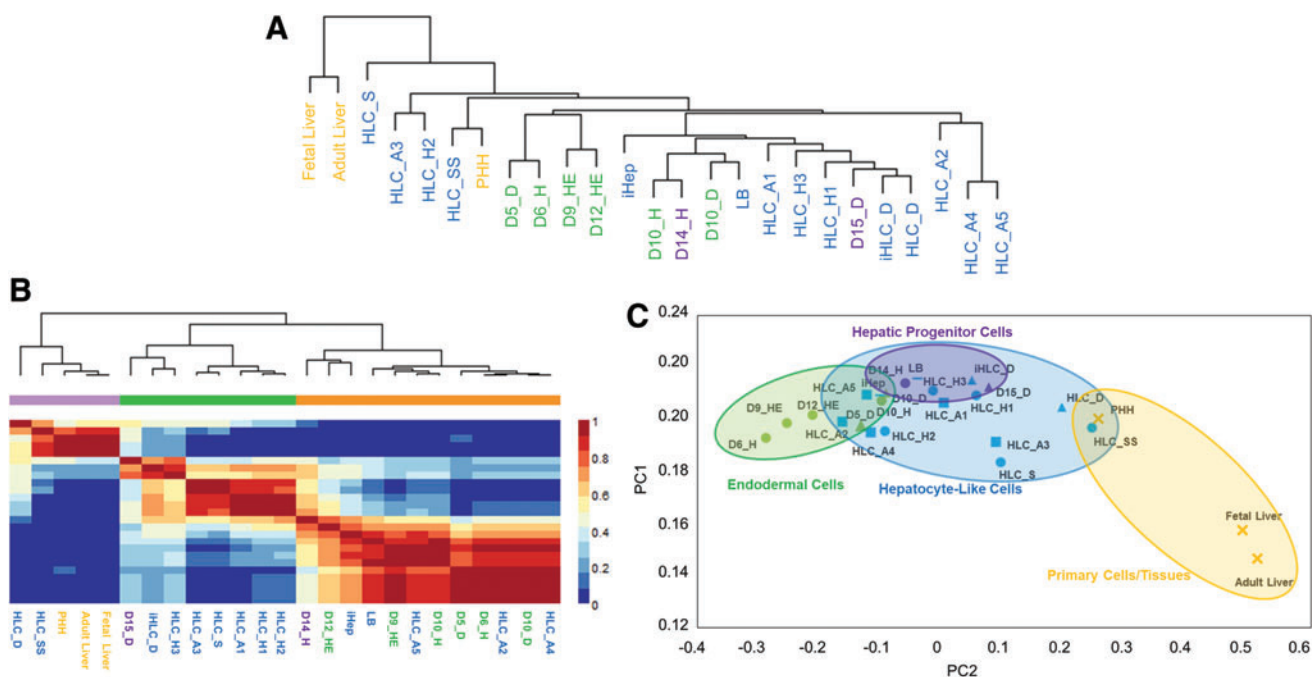
FIG. 1. Clustering of in vitro human differentiation data after batch correction. **(A)** Hierarchical clustering of samples at different stages of differentiation. The colors represent different sources of data. See Supplementary Table S1 for sample annotation. **(B)** NMF on human in vitro data after batch correction. All the samples clustered into three distinct groups of early, mid, and late stages of differentiated cells. **(C)** PCA. The samples aligned according to their differentiation status in the principal component space, starting with endodermal cells followed by HLCs, and the most mature cell types to the far right. The colors represent the different stages of the samples and the shapes represent the different sources of the data. HLCs, hepatocyte-like cells; NMF, non-negative matrix factorization; PCA, principal component analysis; PHHs, primary human hepatocytes. Color images available online at www.liebertpub.com/scd

within a narrow region in the principal component space, suggesting that they all have a similar degree of hepatocyte maturity.

Alignment of the transcriptome of rodent fetal liver development

The data processing pipeline described for the human data sets was used to process the data set of mouse embryonic liver development. The data set compiled from 47 samples across the development of 2 strains of mice was batch corrected [12,33]. A total of 16,415 genes were common across samples based on ENSEMBL ID.

Hierarchical clustering, NMF and PCA, was conducted on the data set. Similar to the observation made before, batch correction removed the bias arising from different platforms and sources (Fig. 2A; Supplementary Fig. S4). Clustering of the samples into two clusters was most optimal, as assessed by the cophenetic coefficient (Supplementary Fig. S5). NMF classified the batch corrected data set into two groups, early and late development, which was in line with the hierarchical clustering results (Fig. 2A, B). When the data were subjected to PCA, the first two principal components captured >90% of the data variance. As was seen for the hPSC-HLC time series, we found that the mouse embryonic liver development samples lined up chronologically in order of their developmental stages (Fig. 2C).

From the NMF and PCA analysis, the samples seemed to be grouped into an early (E9.5–E14.5) cluster and a late

(E15.5–E19.5) cluster. This classification agrees with our understanding of liver development, where the E14.5 stage represents a transition from primarily hematopoiesis to hepatocyte maturation [38]. Functional analysis on the 129 metagenes obtained from the NMF grouping confirmed that genes related to liver functions were key in the grouping of samples (Supplementary Table S4).

Integration of mouse in vitro differentiation and in vivo development data

Transcriptome data of a time course analysis of miPSCs differentiating to HLCs [21] and murine fibroblasts being reprogrammed to iHEPs [39,40] were also compiled and integrated with the mouse embryonic development data sets by batch correction. Again, batch correction removed the bias of platforms, sources and in vitro/in vivo contrast. These combined data were then subjected to PCA. On a plot of PC1 versus PC2, the in vitro differentiation data and in vivo development data can be seen to line up along an arc based on the maturity of the samples, just like the hHLC data (Fig. 3).

The miPSC differentiation data aligned chronologically along E9.5–E15.5 of mouse liver development, while the data points for mouse embryonic liver development beyond E15 continue to spread to the region with higher values of PC2. The results suggest that the miPSC-HLCs and mouse induced hepatocytes (miHEPs) acquired a differentiation stage equivalent of ∼E13.5–E15.5 stage and still lack the maturity of fully developed prenatal E19 and postnatal liver.
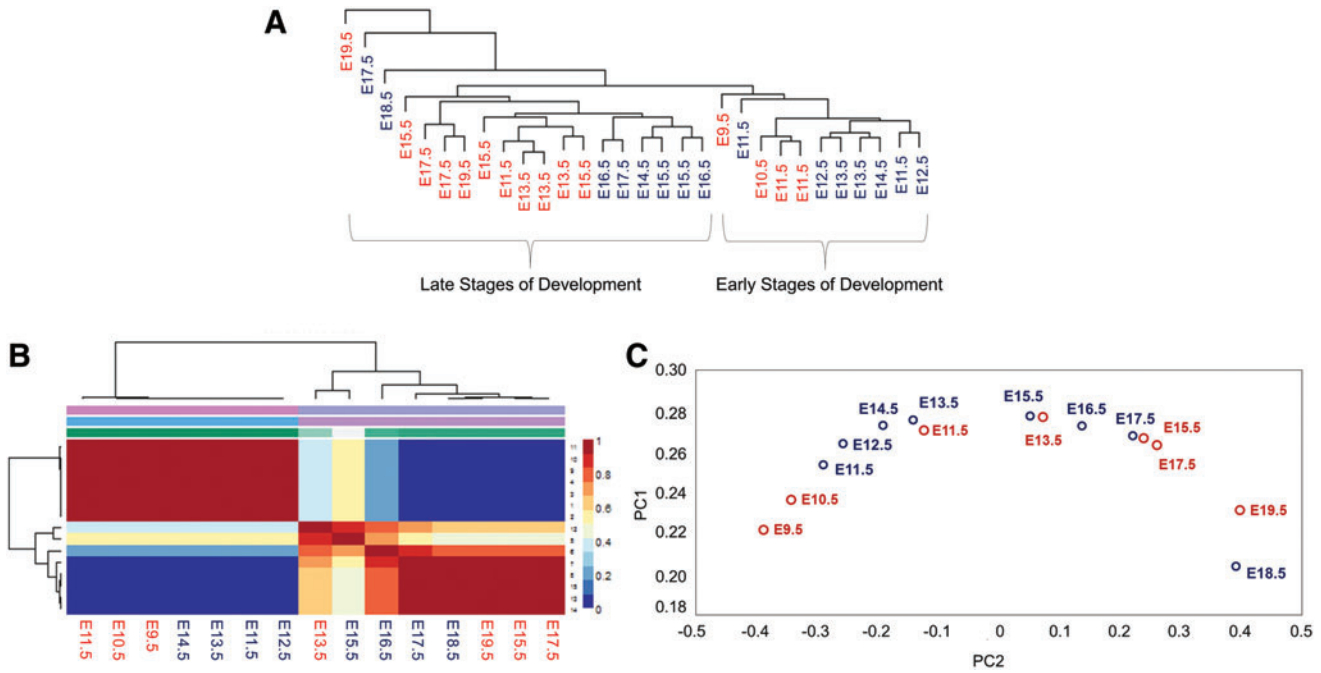
FIG. 2. Clustering of mouse embryonic development data after batch correction. **(A)** Hierarchical clustering grouped different developmental data into early and late stages of development. (*red*): isolated CD34⁻ Ter119⁻ cells from fetal liver (12), (*blue*): cells from a whole liver (33). **(B)** NMF on mouse embryonic development data [biological replicates from **(A)** were averaged] separated the mouse data into two groups of early and late stages of development. **(C)** PCA aligned samples [biological replicates from **(A)** were averaged] according to their developmental stage in the principal component space. Color images available online at www.liebertpub.com/scd

Alignment of mouse in vivo and human in vitro developmental paths

We next integrated the hHLC differentiation data with mouse embryo development data by orthologous genes through common homologous identifiers using the BioMart database package in the statistical program, R. This resulted in a master data set with 14,312 genes. Batch correction was performed on the combined data set to eliminate the batch effects within the samples from different species and in vitro and in vivo samples.

PCA analysis was performed on the integrated data set of hHLC differentiation and mouse embryonic liver development. The data points of mouse and human aligned along the same arc, and lined up in order of their development or hHLC

differentiation stages, respectively (Fig. 4). From the alignment, the corresponding stages of hHLC differentiation and mouse embryo development can be deduced. hPSC-derived endodermal cells were aligned with E9.5–E10.5 samples, and the majority of fully differentiated hHLCs were aligned with E13.5–E15.5 of mouse development. These results strongly indicate that hHLCs derived from hPSCs are more similar to the mouse ∼E14–E15 stage of in vivo development.

Comparison of HLCs with mature cells to find differentially expressed genes

The transcriptome of our day 20 hHLCs and mHLCs was separately compared to their mature counterparts (PHHs and

FIG. 3. Alignment of combined mouse in vitro differentiation and mouse embryonic liver development data. Combined mouse in vitro and in vivo data sets were subjected to PCA and plotted. *Open circles* represent embryonic developmental data, *blue* and *red* indicate samples from two different studies (see Fig. 2). *Closed green circles* represent samples from in vitro differentiation and X represents primary mouse hepatocytes. Color images available online at www.liebert pub.com/scd
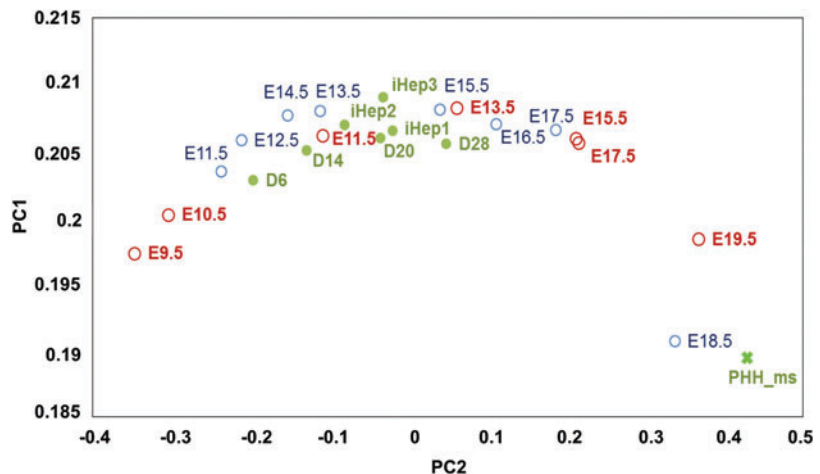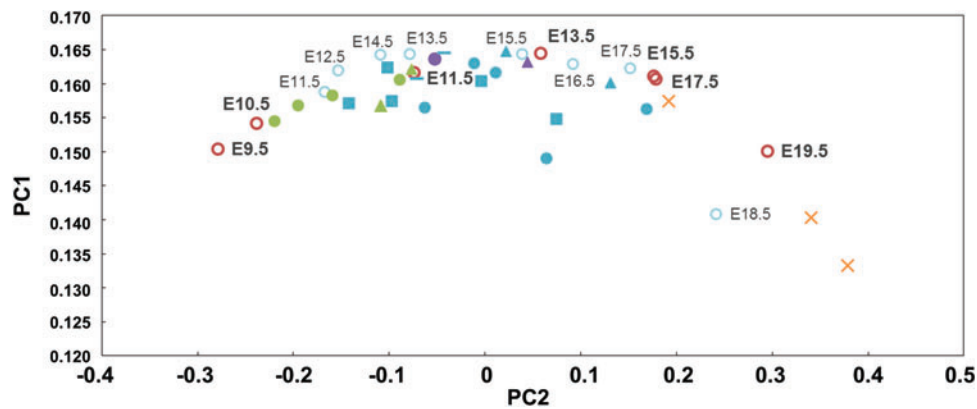
FIG. 4. Alignment of combined human in vitro differentiation and mouse embryonic liver development data. Combined human in vitro and mouse in vivo data sets were subjected to the PCA. The blue and red circles of mouse samples represent two different studies (see Fig. 2). Human in vitro differentiation data are represented by color according to their differentiation state. Endodermal cell, hepatic progenitor cell, and HLC samples are in green, purple, and blue, respectively. The circles, squares, and triangles correspond to samples from references [3,28,31,36]. Color images available online at www.liebertpub.com/scd

E19.5 mouse liver, respectively) using Significance Analysis of Microarray (SAM-R) in R (where the criteria of $q < 0.05$ and fold change >4 were imposed) to identify differentially expressed genes. One hundred twenty-seven genes were identified as differentially expressed between hHLCs and PHHs. Functional analysis on the 127 differentially expressed genes using DAVID revealed that processes involved in *CYP450* drug metabolism, carboxylic acid, amine and lipid metabolism, and complement and coagulation cascades were enriched [37].
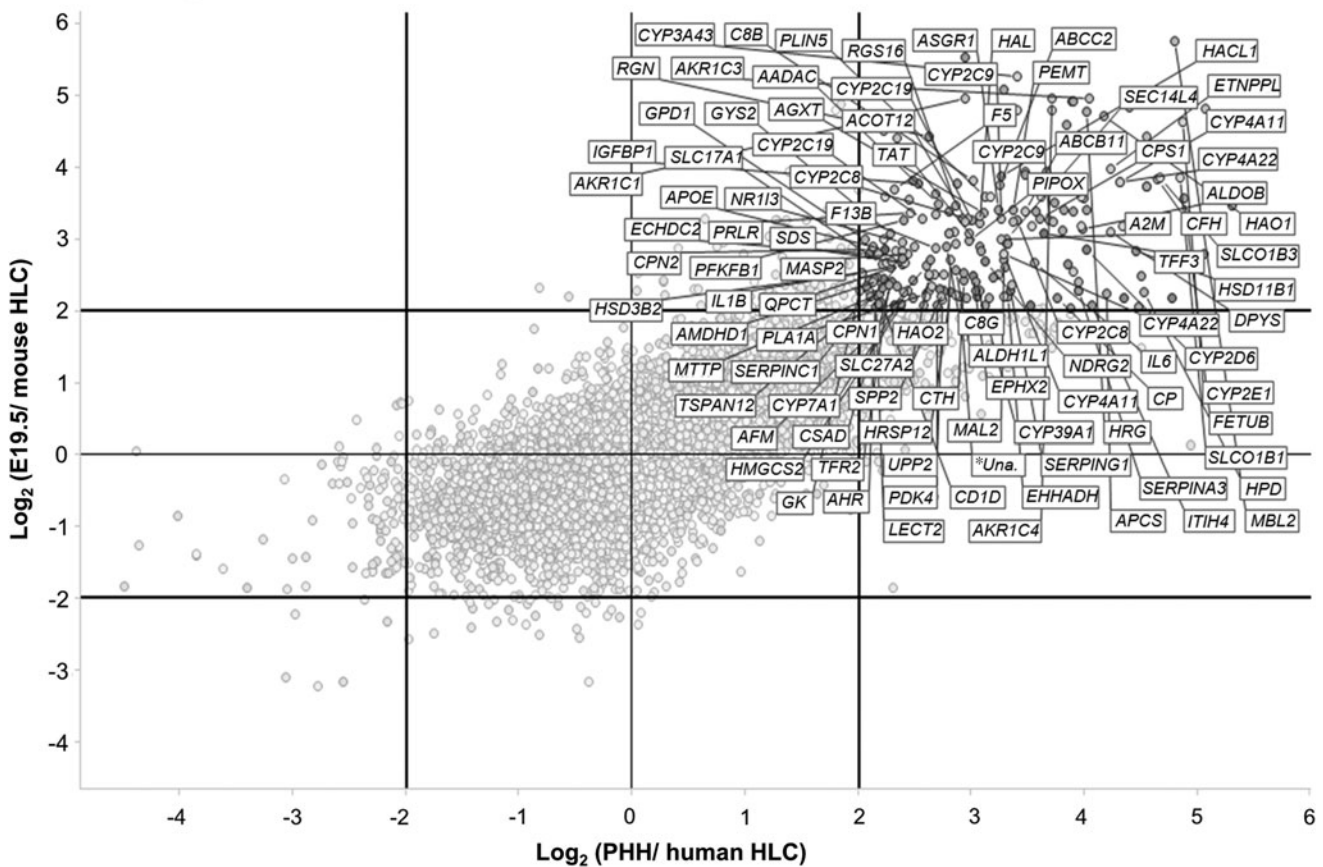
FIG. 5. Differentially expressed genes between HLCs and mature hepatic state (PHH/E19.5). Transcript levels of orthologous genes of human and mouse HLCs were compared to that in E19.5 embryo and PHHs, and plotted against each other. Genes consistently differentially expressed (upregulated by fourfold or higher in E19.5/PHH) in both comparisons were highlighted. *Una.- Unannotated gene.

Among the 127 differentially expressed genes, 42 were common between the human and mouse analyses, which are shown in Figure 5 and listed in Supplementary Table S5. Mature hepatocyte genes that were expressed at low levels in HLCs of both species included metabolic genes, such as *G6PC* and *FBP1*, and the cytochrome *P450* enzymes, *CYP3A4* and *CYP2C9*, indicating the lack of maturity in the metabolic profile of HLCs.

Expression profile comparison on a DT scale

The alignment of hHLC differentiation and mouse embryonic liver development data on a common coordinate grid allowed us to compare the two series of developmental events along a common "time" scale. We treated the arc formed by those data points as a common developmental path. Using the first point (E9.5) as a reference point, the distance of a sample from the reference point along the developmental path can be taken as a "unified developmental time (DT)." A higher value of DT indicates a higher maturity for that sample. The PC2 value of the two time series data of hHLC differentiation (Hu/Duncan) and all the mouse development data (from Fig. 3) was plotted on the DT scale (Fig. 6A). The hHLCs showed a progressive movement along the DT to ∼0.4 (equivalent to ∼E15.5) by the end of the differentiation.

With hHLC differentiation and mouse embryonic liver development on the same DT scale, the similarity or difference in the expression dynamics of any gene can be systematically compared. While some hepatic markers
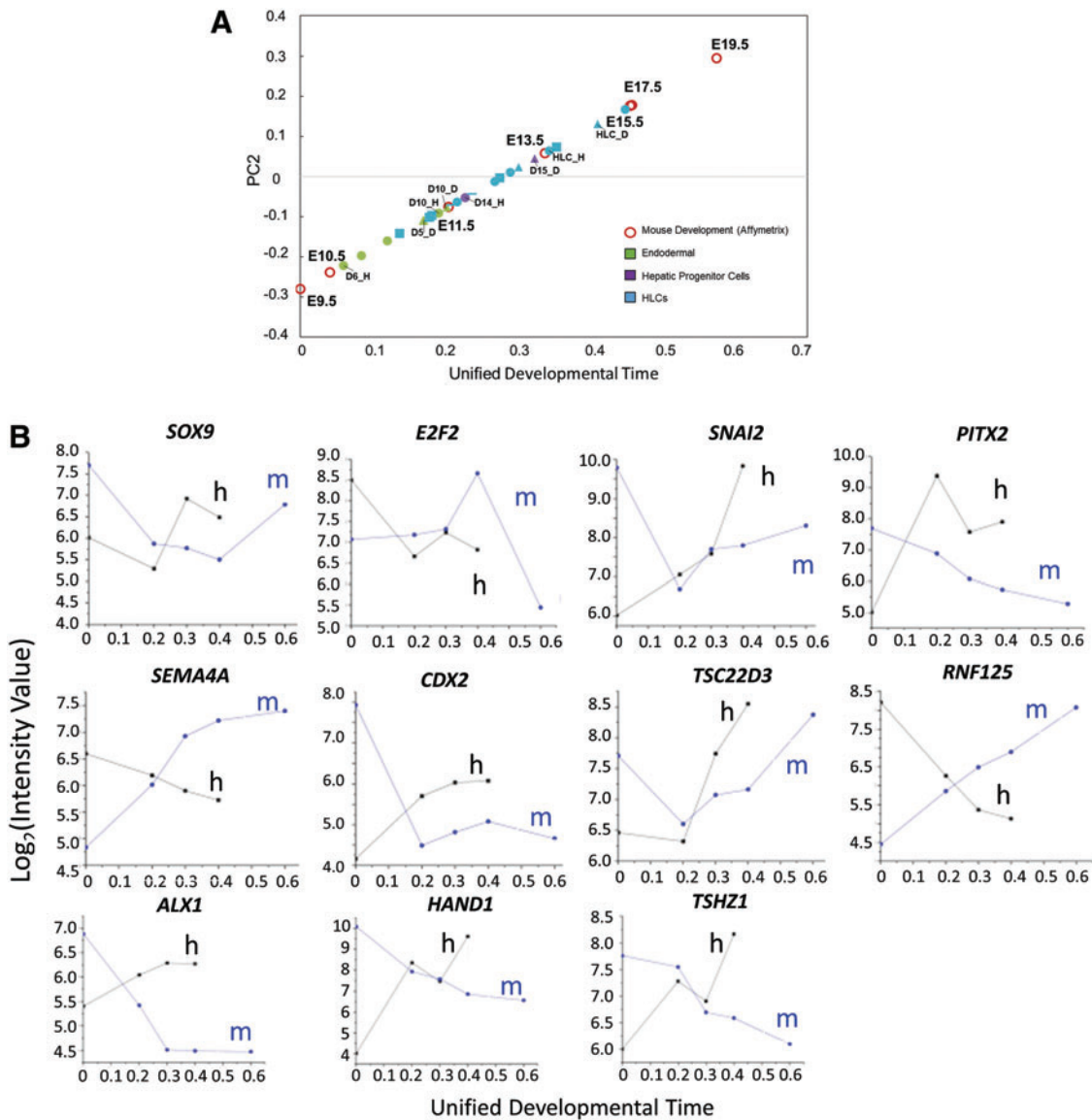
FIG. 6. Alignment of samples along the developmental time and identification of dynamically discordant transcripts. **(A)** Mouse embryo development and human in vitro differentiation samples aligned along DT. The PC2 values for mouse and human samples are plotted against DT. The DT can be represented as a common measure of maturity for in vitro differentiation and in vivo development. **(B)** Cross-species/cross-in vitro-in vivo comparison of transcript dynamics based on DT as a common time scale. Notable transcription factors are plotted along the developmental time. Other discordant transcripts are shown in Supplementary Figure S6. DT, unified developmental time. Color images available online at www.liebertpub.com/scd

(eg, *AFP*) showed similar trends between human in vitro and mouse in vivo data, others showed inconsistent trends.

Dynamic differential expression analysis using Pearson correlation, Spearman's coefficient, and Euclidian distance (PSE) was performed to identify the dynamically differentially expressed genes between mouse development and in vitro differentiation. The Pearson correlation coefficient measures the linear correlation, while the Spearman's coefficient measures the monotonic relationship between two variables. Briefly, the threshold criteria were set for Pearson and Spearman coefficient ≤−0.8 and Euclidean distance ≥μ+2σ, where further details on the criteria imposed are described in the Supplementary Materials and Methods section. The genes fulfilling the PSE criteria were plotted and visually inspected for both human in vitro differentiation and mouse development (Supplementary Fig. S6).

Functional analysis and dynamically differentially expressed gene

One hundred ninety-seven genes were found to be dynamically differentially expressed between hHLC differentiation and mouse embryonic liver development (Supplementary Table S6), including 11 TFs (Fig. 6B), 7 transporters, and 33 other cell surface markers. The major functional classes/pathways involved from the 197 genes identified by the DAVID tool [37] included developmental process, organ development, and cell adhesion as shown in Supplementary Figure S7.

Using the same PSE criteria as before, we identified 141 dynamically differentially expressed genes between mouse embryo liver development and mHLC differentiation (Supplementary Table S7). One hundred one of the 141 genes were common with the 197 genes found in the previous comparison between hHLC differentiation and mouse embryo development. (These genes are marked with * in Supplementary Table S7). The major functional classes/pathways involved from the subset of 101 genes also included developmental process, embryonic morphogenesis, and cell–cell adhesion. This is consistent with the results found previously between hHLC differentiation and mouse embryo development.

Among the 101 consistently discordant genes between mHLC and hHLC are a number of TFs regulating organ development, including *HAND1*, *PITX2*, *ALX1*, *CDX2*, *TSHZ1*, and *SNAI2*. They are found to be highly expressed in the early stages of mouse liver development and subsided after E15, but their transcript levels during hPSC differentiation followed an opposite trend and remained high in hHLCs (Fig. 6B).

We also confirmed the dynamics of the identified differentially expressed TFs, using quantitative reverse transcription-polymerase chain reaction (qRT-PCR) over the course of differentiation (Supplementary Fig. S8). *ALX1* is involved in forebrain development [41], and *CDX2* plays a role in lineage segregation of the inner cell mass and trophectoderm [41,42], as well as intestinal fate and epithelial mesenchymal signaling [43]. *HAND1* regulates embryonic cardiac development [44], *PITX2* participates in limb development [45,46], *SOX9* in pancreatic and bile duct development [47], *SNAI2* in epithelial–mesenchymal transition (EMT) [48,49], and *TSHZ1* in pancreatic cell development and maturation [50]. We examined the TF binding sites in the promoter regions of the dynamically differentially expressed genes (http://genome.ucsc .edu/ENCODE/). The TFs that have their binding site present in the promoter region of the most differentially expressed genes are listed in Supplementary Table S8.

Several cell surface proteins also had opposite trends of transcript dynamics between HLC differentiation and mouse liver development (Supplementary Fig. S6), including *SPARC*, an extracellular matrix secreted factor, and *CDH3* (P-cadherin). Their transcript levels increased during differentiation, but decreased in the developing embryonic mouse liver. Comparison of the expression levels of the hepatic markers, alpha-fetoprotein (*AFP*) and albumin (*ALB*), for mouse development and our time series in vitro human differentiation (Hu) (Supplementary Fig. S9A–C) revealed consistent trends and similar magnitudes of gene expression dynamics before and after batch correction. The profile of all 197 dynamically differentially expressed genes was also visually inspected after plotting with TimeVIEW to affirm that treatment with ComBat did not distort the data (Supplementary Fig. S10) [51].

Discussion

In this study, we used highly heterogeneous transcriptome data from hPSC and mPSC in vitro differentiation and mouse in vivo embryo development for meta-analysis. Batch corrections were performed on the data to remove systematic variations biasing our observations. Previous studies have shown that the empirical Bayes-based ComBat algorithm can be relied on in removing system bias caused by a mixture of transcriptome data from different populations of cells of different sources [52–57]. ComBat had previously been shown to integrate transcriptome data from multiple studies of different vascular endothelial growth factor (*VEGF*) isoform mice to identify the role *VEGF* plays in neural stem cell fate [52].

Recently, ComBat was used for treating the transcriptome data of different PSC populations generated from multiple studies to determine the similarities between genetically matched iPSCs, nuclear transfer stem cells, and embryonic stem cells [56]. We extended its use for combining data from different species and across the in vitro/in vivo to understand stem cell hepatocyte differentiation. Through successive data processing with increasing level of data complexity, we successfully integrated hPSC-HLC differentiation data from different studies with mouse in vivo liver development data.

In each level of analysis, after batch correction, unsupervised clustering grouped the different samples by their biological similarities instead of the source of the sample (Figs. 1 and 2; Supplementary Figs. S2 and S4). The clustering and functional analysis of the batch-corrected data reveal the biological similarities between the different samples after data processing. In addition, the functional classes of the metagene obtained in NMF were found to be related to development and liver functions, confirming the biological relevance from clustering of the samples. Importantly, the genes we identified as dynamically differentially expressed retained the same dynamics before and after batch correction.

Identification of similar stages of development across different species that have vastly different time scales often relies on common morphological, biochemical, and genetic hallmarks. For example, in human embryo, development days 22 and 52 are considered to be equivalent to mouse E9.5 and E14.5, respectively [58]. In an earlier study, neural development events were used to generate a regression model

for predicting a time table of corresponding stages across nine species [59]. Recently, transcriptome data of nematode species were compared to morphological markers to establish embryo developmental milestones in different species of *Caenorhabditis* [60]. In another study, different feature measurements of leaves for different tomato species were subjected to PCA to establish a developmental trajectory [61].

Similarly, RNA-seq data of a species' developing embryo were subjected to PCA to align the developmental stage in the PC plane [62]. However, in many cases, the maturity of HLCs is measured by comparing it to primary hepatocytes at the functional, proteome, and transcriptome level. To our knowledge, this is the first study to compare genes across species and across the in vitro/in vivo border in a dynamic manner to identify the developmental stage which HLCs are stuck at.

Our meta-analysis revealed that HLCs were closer to mid-liver development ($\sim$E15.5) than to primary adult hepatocytes. This indicates that irrespective of the species of origin, or the protocols used, differentiating HLCs appear to encounter universal roadblocks preventing their maturation. It also suggests that there might be a fundamental block that prevents HLCs from maturing further.

Using the common scale that was developed, we can align the transcript dynamics of human in vitro PSC-HLC differentiation with mouse in vivo development to identify genes whose expression was progressing in the wrong direction compared to the in vivo processes. We also identified differentially expressed genes between h/mHLCs and mature cells (E19.5, adult liver), including key *CYP450* enzymes (*CYP2C8*, *CYP2C9*, *CYP2E1*, *CYP2D6*, and *CYP3A4*) and metabolic isozymes (*ALDOB*, *GLUT2*, *G6PC*, and *FBP1*), which are all hallmarks of mature liver metabolism.

The 197 dynamically differentially expressed genes between hHLC differentiation and mouse liver embryo development similarly pointed to the lack of maturity in HLCs. An example is the expression of genes involved in the glucose metabolism. As hepatocytes become more mature, a new set of transporters, enzymes, and their isoforms in glucose metabolism is expressed to give the liver its capability in maintaining the homeostasis of glucose and gluconeogenesis. Notably, the increased expression of glucose transporter *GLUT2*, and aldolase B (*ALDOB*) seen in mouse liver development and human adult hepatocytes did not yet occur in HLCs (Supplementary Fig. S11). Not surprisingly, the increased expression of the gluconeogenesis enzymes, glucose 6-phosphatase (*G6PC*) and fructose 1,6-biphosphatase (*FBP*), seen in mouse development was also not seen in HLCs.

Since both hHLCs and mHLCs ceased further maturation at about E14–E15 stage, it is plausible that they face the same genetic barriers. The ''discordant'' behavior of some of the common dynamically differentially expressed genes identified may have contributed to the lack of further maturation. One hundred one genes were identified as having discordant behavior in both species of HLC differentiation compared to mouse embryo liver development. Some of the common TFs identified are not known to play a role in liver development, but are involved in the development of heart (*HAND1*), eye, or lung (*SOX9*) [63]. Although this may not be surprising, as hepatocytes are created by a mesendodermal precursor early during development, persistent expression of these TFs may prevent final maturation of HLCs to the level of primary hepatocytes.

Furthermore, TGFβ signaling in conjunction with upregulation of *SNAI2* is consistent with EMT, which has been described previously as being abnormally expressed in HLCs compared with PHHs [48]. The opposing trend of transcript dynamics of these TFs may be indicative of discordant gene regulation between mouse liver development and HLC differentiation.

The gene expression profile and metabolic activities have led to the notion that HLCs were closer to fetal than adult hepatocytes [10]. Another study of comparison between HLCs and human hepatocytes at the transcriptome level revealed 4,000 differentially expressed genes [9]. Our study demonstrates for the first time that HLCs obtained using various protocols and from different sources are all equivalent to E13–E15.5 of mouse development. We could pin point the stage of developmental block by developing a ''unified developmental time'' that can span across species and in vitro and in vivo samples.

Despite the difference in the methodology used, a large fraction of genes identified as differentially expressed in the previous studies [9,10] was also identified as dynamically differentially expressed in our study (Supplementary Fig. S12). However, differences between the two studies are also seen. Given the different reference of comparison used (time course of embryonic liver development in this study versus primary hepatocytes in [9,10]), some differences in the differentially expressed gene list are not surprising. Instead of measuring the maturity of HLCs using the expression level of mature markers, the dynamic profile of the differentiation transcriptome was used. We identified not only the liver markers that should be expressed at high levels but also certain genes that might need to be suppressed.

This study reaffirmed that HLCs are at an immature hepatocyte cell state, and for the first time identifies the ''corresponding stage'' during embryonic liver development. Many genes whose expression followed a different pattern from that in the developing embryo might contribute to this block in further maturation. Whether inhibition of misexpressed TFs and activation of TFs that are missing will enhance maturation of stem cell-derived hepatocytes remains to be determined. In addition, this meta-analysis pipeline should be applicable to PSC differentiation studies to other lineages if the time course transcriptome data for both in vitro differentiation and in vivo development are available.

Author Disclosure Statement

No competing financial interests exist.

References

1. Haridass D, N Narain and M Ott. (2008). Hepatocyte transplantation: waiting for stem cells. Curr Opin Organ Transplant 13:627–632.
2. Roelandt P, KA Pauwelyn, P Sancho-Bru, K Subramanian, B Bose, L Ordovas, K Vanuytsel, M Geraerts, M Firpo,

et al. (2010). Human embryonic and rat adult stem cells with primitive endoderm-like phenotype can be fated to definitive endoderm, and finally hepatocyte-like cells. PLoS One 5:e12101.

3. Jozefczuk J, A Prigione, L Chavez and J Adjaye. (2011). Comparative analysis of human embryonic stem cell and induced pluripotent stem cell-derived hepatocyte-like cells reveals current drawbacks and possible strategies for improved differentiation. Stem Cells Dev 20:1259–1275.

4. Chamberlain J, T Yamagami, E Colletti, ND Theise, J Desai, A Frias, J Pixley, ED Zanjani, CD Porada and G Almeida-Porada. (2007). Efficient generation of human hepatocytes by the intrahepatic delivery of clonal human mesenchymal stem cells in fetal sheep. Hepatology 46: 1935–1945.

5. Qian H, J Wang, S Wang, Z Gong, M Chen, Z Ren and S Huang. (2006). In utero transplantation of human hematopoietic stem/progenitor cells partially repairs injured liver in mice. Int J Mol Med 18:633–642.

6. Basma H, A Soto-Gutiérrez, GR Yannam, L Liu, R Ito, T Yamamoto, E Ellis, SD Carson, S Sato, et al. (2009). Differentiation and transplantation of human embryonic stem cell-derived hepatocytes. Gastroenterology 136:990–999.

7. Avital I, D Inderbitzin, T Aoki, DB Tyan, AH Cohen, C Ferraresso, J Rozga, WS Arnaout and AA Demetriou. (2001). Isolation, characterization, and transplantation of bone marrow-derived hepatocyte stem cells. Biochem Biophys Res Commun 288:156–164.

8. Moreno R, I Martínez-González, M Rosal, M Nadal, J Petriz, E Gratacós and JM Aran. (2012). Fetal liver-derived mesenchymal stem cell engraftment after allogeneic in utero transplantation into rabbits. Stem Cells Dev 21:284–295.

9. Godoy P, W Schmidt-Heck, K Natarajan, B Lucendo-Villarin, D Szkolnicka, A Asplund, P Björquist, A Widera, R Stöber, et al. (2015). Gene networks and transcription factor motifs defining the differentiation of stem cells into hepatocyte-like cells. J Hepatol 63:934–942.

10. Baxter M, S Withey, S Harrison, CP Segeritz, F Zhang, R Atkinson-Dell, C Rowe, DT Gerrard, R Sison-Young, et al. (2015). Phenotypic and functional analyses show stem cell-derived hepatocyte-like cells better mimic fetal rather than adult hepatocytes. J Hepatol 62:581–589.

11. Subramanian K, DJ Owens, R Raju, M Firpo, TD O'Brien, CM Verfaillie and WS Hu. (2014). Spheroid culture for enhanced differentiation of human embryonic stem cells to hepatocyte-like cells. Stem Cells Dev 23:124–131.

12. Takebe T, K Sekine, M Enomura, H Koike, M Kimura, T Ogaeri, RR Zhang, Y Ueno, YW Zheng, et al. (2013). Vascularized and functional human liver from an iPSC-derived organ bud transplant. Nature 499:481–484.

13. Soto-Gutiérrez A, N Navarro-Alvarez, D Zhao, JD Rivas-Carrillo, J Lebkowski, N Tanaka, IJ Fox and N Kobayashi. (2007). Differentiation of mouse embryonic stem cells to hepatocyte-like cells by co-culture with human liver non-parenchymal cell lines. Nat Protoc 2:347–356.

14. Du C, K Narayanan, MF Leong and AC Wan. (2014). Induced pluripotent stem cell-derived hepatocytes and endothelial cells in multi-component hydrogel fibers for liver tissue engineering. Biomaterials 35:6006–6014.

15. Shan J, RE Schwartz, NT Ross, DJ Logan, D Thomas, SA Duncan, TE North, W Goessling, AE Carpenter and SN Bhatia. (2013). Identification of small molecules for human

hepatocyte expansion and iPS differentiation. Nat Chem Biol 9:514–520.

16. Tasnim F, D Phan, YC Toh and H Yu. (2015). Cost-effective differentiation of hepatocyte-like cells from human pluripotent stem cells using small molecules. Biomaterials 70:115–125.

17. Siller R, S Greenhough, E Naumovska and GJ Sullivan. (2015). Small-molecule-driven hepatocyte differentiation of human pluripotent stem cells. Stem Cell Rep 4:939–952.

18. Takayama K, M Inamura, K Kawabata, K Katayama, M Higuchi, K Tashiro, A Nonaka, F Sakurai, T Hayakawa, MK Furue and H Mizuguchi. (2012). Efficient generation of functional hepatocytes from human embryonic stem cells and induced pluripotent stem cells by HNF4alpha transduction. Mol Ther 20:127–137.

19. Takayama K, M Inamura, K Kawabata, M Sugawara, K Kikuchi, M Higuchi, Y Nagamoto, H Watanabe, K Tashiro, et al. (2012). Generation of metabolically functioning hepatocytes from human pluripotent stem cells by FOXA2 and HNF1alpha transduction. J Hepatol 57:628–636.

20. Du Y, J Wang, J Jia, N Song, C Xiang, J Xu, Z Hou, X Su, B Liu, et al. (2014). Human hepatocytes with drug metabolic function induced from fibroblasts by lineage reprogramming. Cell Stem Cell 14:394–403.

21. Sancho-Bru P, P Roelandt, N Narain, K Pauwelyn, T Notelaers, T Shimizu, M Ott and C Verfaillie. (2011). Directed differentiation of murine-induced pluripotent stem cells to functional hepatocyte-like cells. J Hepatol 54:98–107.

22. Johnson WE, C Li and A Rabinovic. (2007). Adjusting batch effects in microarray expression data using empirical Bayes methods. Biostatistics 8:118–127.

23. Sims AH, GJ Smethurst, Y Hey, MJ Okoniewski, SD Pepper, A Howell, CJ Miller and RB Clarke. (2008). The removal of multiplicative, systematic bias allows integration of breast cancer gene expression datasets—improving meta-analysis and prediction of prognosis. BMC Med Genomics 1:42.

24. Chen C, K Grennan, J Badner, D Zhang, E Gershon, L Jin and C Liu. (2011). Removing batch effects in analysis of expression microarray data: an evaluation of six batch adjustment methods. PLoS One 6:e17238.

25. Nygaard V, EA Rødland and E Hovig. (2016). Methods that remove batch effects while retaining group differences may lead to exaggerated confidence in downstream analyses. Biostatistics 17:29–39.

26. Benito M, J Parker, Q Du, J Wu, D Xiang, CM Perou and JS Marron. (2004). Adjustment of systematic microarray data biases. Bioinformatics 20:105–114.

27. Luo J, M Schumacher, A Scherer, D Sanoudou, D Megherbi, T Davison, T Shi, W Tong, L Shi, et al. (2010). A comparison of batch effect removal methods for enhancement of prediction performance using MAQC-II microarray gene expression data. Pharmacogenomics J 10:278–291.

28. DeLaForest A, M Nagaoka, K Si-Tayeb, FK Noto, G Konopka, MA Battle and SA Duncan. (2011). HNF4A is essential for specification of hepatic progenitors from human pluripotent stem cells. Development 138:4143–4153.

29. Roelandt P, S Obeid, J Paeshuyse, J Vanhove, A Van Lommel, Y Nahmias, F Nevens, J Neyts and CM Verfaillie. (2012). Human pluripotent stem cell-derived hepatocytes support complete replication of hepatitis C virus. J Hepatol 57:246–251.

30. Touboul T, NR Hannan, S Corbineau, A Martinez, C Martinet, S Branchereau, S Mainot, H Strick-Marchand,

R Pedersen, et al. (2010). Generation of functional hepatocytes from human embryonic stem cells under chemically defined conditions that recapitulate liver development. Hepatology 51:1754–1765.

31. Si-Tayeb K, FK Noto, M Nagaoka, J Li, MA Battle, C Duris, PE North, S Dalton and SA Duncan. (2010). Highly efficient generation of human hepatocyte-like cells from induced pluripotent stem cells. Hepatology 51:297–305.

32. Huang P, L Zhang, Y Gao, Z He, D Yao, Z Wu, J Cen, X Chen, C Liu, et al. (2014). Direct reprogramming of human fibroblasts to functional and expandable hepatocytes. Cell Stem Cell 14:370–384.

33. Li T, J Huang, Y Jiang, Y Zeng, F He, MQ Zhang, Z Han and X Zhang. (2009). Multi-stage analysis of gene expression and transcription regulation in C57/B6 mouse liver development. Genomics 93:235–242.

34. Heider A and R Alt. (2013). virtualArray: a R/bioconductor package to merge raw data from different microarray platforms. BMC Bioinformatics 14:75.

35. Durinck S, PT Spellman, E Birney and W Huber. (2009). Mapping identifiers for the integration of genomic datasets with the R/Bioconductor package biomaRt. Nat Protoc 4:1184–1191.

36. Raju R, D Chau, DS Cho, Y Park, CM Verfaillie and WS Hu. (2017). Cell expansion during directed differentiation of stem cells toward the hepatic lineage. Stem Cells Dev 26:274–284.

37. Huang W, BT Sherman and RA Lempicki. (2009). Bioinformatics enrichment tools: paths toward the comprehensive functional analysis of large gene lists. Nucleic Acids Res 37:1–13.

38. Hegedűs T, G Gyimesi, ME Gáspár, KZ Szalay, R Gangal and P Csermely. (2013). Potential application of network descriptions for understanding conformational changes and protonation states of ABC transporters. Curr Pharm Des 19:4155–4172.

39. Huang P, Z He, S Ji, H Sun, D Xiang, C Liu, Y Hu, X Wang and L Hui. (2011). Induction of functional hepatocyte-like cells from mouse fibroblasts by defined factors. Nature 475:386–389.

40. Sekiya S and A Suzuki. (2011). Direct conversion of mouse fibroblasts to hepatocyte-like cells by defined factors. Nature 475:390–393.

41. Nelms BL and PA Labosky. (2010). *Transcriptional Control of Neural Crest Development*. Morgan & Claypool Life Sciences, San Rafael, CA.

42. Strumpf D, CA Mao, Y Yamanaka, A Ralston, K Chawengsaksophak, F Beck and J Rossant. (2005). Cdx2 is required for correct cell fate specification and differentiation of trophectoderm in the mouse blastocyst. Development 132:2093–2102.

43. Gao N, P White and KH Kaestner. (2009). Establishment of intestinal identity and epithelial-mesenchymal signaling by Cdx2. Dev Cell 16:588–599.

44. McFadden DG, AC Barbosa, JA Richardson, MD Schneider, D Srivastava and EN Olson. (2005). The Hand1 and Hand2 transcription factors regulate expansion of the embryonic cardiac ventricles in a gene dosage-dependent manner. Development 132:189–201.

45. Duboc V and MP Logan. (2011). Pitx1 is necessary for normal initiation of hindlimb outgrowth through regulation of Tbx4 expression and shapes hindlimb morphologies via targeted growth control. Development 138:5301–5309.

46. Bensoussan-Trigano V, Y Lallemand, C Saint Cloment and B Robert. (2011). Msx1 and Msx2 in limb mesenchyme modulate digit number and identity. Dev Dyn 240:1190–1202.

47. Belo J, M Krishnamurthy, A Oakie and R Wang. (2013). The role of SOX9 transcription factor in pancreatic and duodenal development. Stem Cells Dev 22:2935–2943.

48. Casas E, J Kim, A Bendesky, L Ohno-Machado, CJ Wolfe and J Yang. (2011). Snail2 is an essential mediator of Twist1-induced epithelial mesenchymal transition and metastasis. Cancer Res 71:245–254.

49. Fenouille N, M Tichet, M Dufies, A Pottier, A Mogha, JK Soo, S Rocchi, A Mallavialle, MD Galibert, et al. (2012). The epithelial-mesenchymal transition (EMT) regulatory factor SLUG (SNAI2) is a downstream target of SPARC and AKT in promoting melanoma cell invasion. PLoS One 7:e40378.

50. Raum JC, SA Soleimanpour, DN Groff, N Coré, L Fasano, AN Garratt, C Dai, AC Powers and DA Stoffers. (2015). Tshz1 Regulates Pancreatic β-Cell Maturation. Diabetes 64:2905–2914.

51. Gadgil M, S Mehra, V Kapur and WS Hu. (2006). Time-View: for comparative gene expression analysis. Appl Bioinformatics 5:41–44.

52. Cain JT, MA Berosik, SD Snyder, NF Crawford, SI Nour, GJ Schaubhut and DC Darland. (2014). Shifts in the vascular endothelial growth factor isoforms result in transcriptome changes correlated with early neural stem cell proliferation and differentiation in mouse forebrain. Dev Neurobiol 74:63–81.

53. Gentles AJ, AM Newman, CL Liu, SV Bratman, W Feng, D Kim, VS Nair, Y Xu, A Khuong, et al. (2015). The prognostic landscape of genes and infiltrating immune cells across human cancers. Nat Med 21:938–945.

54. Müller C, A Schillert, C Röthemeier, DA Trégouët, C Proust, H Binder, N Pfeiffer, M Beutel, KJ Lackner, et al. (2016). Removing batch effects from longitudinal gene expression—quantile normalization plus ComBat as best approach for microarray transcriptome data. PLoS One 11:e0156594.

55. Miller JA, SL Ding, SM Sunkin, KA Smith, L Ng, A Szafer, A Ebbert, ZL Riley, JJ Royall, et al. (2014). Transcriptional landscape of the prenatal human brain. Nature 508:199–206.

56. Ma H, R Morey, RC O'Neil, Y He, B Daughtry, MD Schultz, M Hariharan, JR Nery, R Castanon, et al. (2014). Abnormalities in human pluripotent cells due to reprogramming mechanisms. Nature 511:177–183.

57. Rempel E, L Hoelting, T Waldmann, NV Balmer, S Schildknecht, M Grinberg, JA Das Gaspar, V Shinde, R Stöber, et al. (2015). A transcriptome-based classifier to identify developmental toxicants by stem cell testing: design, validation and optimization for histone deacetylase inhibitors. Arch Toxicol 89:1599–1618.

58. Downs KM and T Davies. (1993). Staging of gastrulating mouse embryos by morphological landmarks in the dissecting microscope. Development 118:1255–1266.

59. Clancy B, RB Darlington and BL Finlay. (2001). Translating developmental time across mammalian species. Neuroscience 105:7–17.

60. Levin M, T Hashimshony, F Wagner and I Yanai. (2012). Developmental milestones punctuate gene expression in the Caenorhabditis embryo. Dev Cell 22:1101–1108.

61. Chitwood DH, LR Headland, R Kumar, J Peng, JN Maloof and NR Sinha. (2012). The developmental trajectory of leaflet morphology in wild tomato species. Plant Physiol 158:1230–1240.

62. Anavy L, M Levin, S Khair, N Nakanishi, SL Fernandez-Valverde, BM Degnan and I Yanai. (2014). BLIND ordering of large-scale transcriptomic developmental time courses. Development 141:1161–1166.

63. Rockich BE, SM Hrycaj, HP Shih, MS Nagy, MA Ferguson, JL Kopp, M Sander, DM Wellik and JR Spence. (2013). Sox9 plays multiple roles in the lung epithelium during branching morphogenesis. Proc Natl Acad Sci U S A 110:E4456–E4464.

Address correspondence to:
Dr. Wei-Shou Hu
Department of Chemical Engineering and Materials Science
University of Minnesota
421 Washington Avenue SE
Minneapolis, MN 55455-0132

E-mail: acre@cems.umn.edu